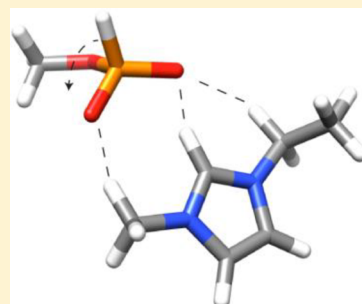


Physical Properties, Ion–Ion Interactions, and Conformational States of Ionic Liquids with Alkyl-Phosphonate Anions

Jagath Pitawala, Johan Scheers, Per Jacobsson, and Aleksandar Matic*

Department of Applied Physics, Chalmers University of Technology, SE-412 96 Göteborg, Sweden

ABSTRACT: We investigate the ionic conductivities, phase behaviors, conformational states, and interactions of three ionic liquids based on imidazolium cations and phosphonate anions with varying alkyl chain lengths. All three ionic liquids show high conductivities, with 1,3-dimethylimidazolium methyl-phosphonate [DiMIm(MeO)(H)-PO₂] being the most conductive ($7.3 \times 10^{-3} \text{ S cm}^{-1}$ at 298 K). The high ionic conductivities are a result of the low glass-transition temperatures, T_g , which do not change significantly upon changing the cation and/or anion size. However, there is a slight dependence of the temperature behavior of the conductivity on the size of the ions, as seen from the fragility parameter (D) obtained from fits to the Vogel–Fulcher–Tammann equation. The molecular-level structure and interactions of the phosphonate anions were examined by Raman spectroscopy and first-principles calculations. The calculations identify two stable conformations for the methyl- and ethyl-phosphonate anions by rotation of the methyl and ethyl groups, respectively. The broad Raman signatures of the anions suggest the coexistence of two anion conformers in the ionic liquids and non-negligible cation–anion interactions, with a dependence on the position and shape of the bands of the cation species and the alkyl group of the anion.



1. INTRODUCTION

Ionic liquids (ILs) are defined as materials entirely composed of ions that have a melting point below 100 °C.¹ They typically consist of large organic cations (e.g., imidazolium, pyrrolidinium, pyridinium, and quaternary ammonium) and charge-delocalized anions (e.g., BF₄[−], PF₆[−], N(SO₂CF₃)₂[−], and N(SO₂F)₂[−]). Combining all possible cations and anions allows the formation of a large number of ILs with properties of interest in many applications, such as high ionic conductivity, high thermal and electrochemical stability, nonflammability, nonvolatility, and a wide temperature range of the liquid state.² An understanding of the relation between the molecular structure of ILs and their physical properties is the basis for the rational design of new ILs having tailored properties. The cationic structure is generally changed by introducing alkyl side chains of different lengths.^{3–7} On the anion side, the size and shape can also be changed, as can the extent of charge delocalization.^{8–10}

There are some reports on the dependence of the physicochemical properties of ILs on the anion.^{11–16} Most of the studies are focused on fluorinated anions, and less attention has been paid to nonfluorinated species. The general problem of fluorine-rich anions, such as tetrafluoroborate (BF₄[−]) and hexafluorophosphate (PF₆[−]), is their low chemical stability, particularly toward hydrolysis, which limits their applicability under moisture-free conditions.¹⁷ The decomposition of halogen-containing ILs may result in the release of toxic and corrosive hydrogen halides to the surrounding environment.¹⁸ To mitigate these problems, water-stable ILs with fluorinated anions, such as bis(trifluoromethanesulfonyl)imide (TFSI), have been developed.¹⁹ However, many ILs with the TFSI anion and small cations crystallize easily, which limits the liquid

range.^{20–22} Crystallization can be avoided by the introduction of longer alkyl chains on the cation; however, as a result of this introduction the viscosity increases and conductivity decreases.⁴ Thus, although the physical properties of some ILs composed of fluorine-free anions have been reported, the synthesis and characterization of new environmental friendly ILs is needed.^{17,18,23–26}

In this Article, we report on the physical properties, interactions, and conformational states of ILs that are based on the rather new phosphonate anions and traditional imidazolium cations. The names, acronyms, and molecular structures of the novel ILs are given in Figure 1. We compare our results with those of two well-established ILs, 1-ethyl-3-methylimidazolium bis(trifluoromethanesulfonyl)-imide (EMImTFSI) and 1-ethyl-3-methylimidazolium tetrafluoroborate (EMImBF₄). These two ILs have the same cation as the phosphonate ILs under investigation; therefore, the anion influence on the properties of these ILs can be addressed. We have investigated transport properties (i.e., ionic conductivity) by dielectric spectroscopy and phase behavior by differential scanning calorimetry (DSC). The structures of the phosphonate anions were examined by Raman spectroscopy and ab initio calculations.

2. EXPERIMENTAL SECTION

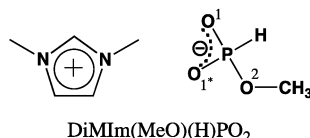
2.1. Materials. The phosphonate anion-based ionic liquids 1,3-dimethylimidazolium methyl-phosphonate [(DiMIm-

Received: February 7, 2013

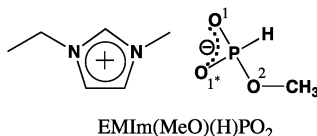
Revised: June 17, 2013

Published: June 17, 2013

1,3-Dimethylimidazolium Methyl-Phosphonate



1-Ethyl-3-methylimidazolium Methyl-Phosphonate



1-Ethyl-3-methylimidazolium Ethyl-Phosphonate

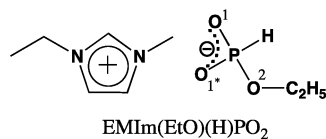


Figure 1. Names, acronyms, and molecular structures of the investigated ionic liquids. The anion oxygen atoms are denoted by the numbers 1, 1*, and 2 to distinguish the different anion conformers. The dotted line shows the charge delocalization on the O(1*)–P–O(1) part of the anion.

(MeO)(H)PO₂], 1-ethyl-3-methylimidazolium methyl-phosphonate [(EMIm(MeO)(H)PO₂)], and 1-ethyl-3-methylimidazolium ethyl-phosphonate [(EMIm(EtO)(H)PO₂)] (>98%) were obtained from Solvionic. 1-Ethyl-3-methylimidazolium bis(trifluoromethanesulfonyl)imide (EMImTFSI) and 1-ethyl-3-methylimidazolium tetrafluoroborate (EMImBF₄) (>99%) were obtained from Sigma-Aldrich. All samples were stored and handled in an argon drybox (oxygen and water of less than 1 ppm) and used as received.

2.2. Characterization Methods. The temperature dependence of the ionic conductivity was measured by dielectric spectroscopy using a Novocontrol broadband dielectric spectrometer in the frequency range of 10^{−1}–10⁷ Hz. The samples were placed between stainless steel electrodes with a Teflon spacer, defining the sample as 13 mm in diameter and 1 mm in thickness. The conductivity cell was assembled in an argon drybox and loaded into a cryo-furnace. Data were collected upon cooling in steps of 10 K, with a 15 min thermal equilibration at each temperature, in the temperature range of 383–243 K. A steady flow of nitrogen gas was supplied to the sample holder to maintain a dry atmosphere. The dc conductivity was extracted as the low-frequency plateau in the frequency-dependent conductivity plot.

Differential scanning calorimetry (DSC) experiments were performed using a Q1000 (TA Instruments). The samples were placed in hermetically sealed aluminum pans. The DSC experiments were performed as follows. After their equilibration at 313 K, the samples were cooled to 133 K using a cooling rate of 20 K/min. Thereafter, the samples were equilibrated at 133 K and subsequently heated from 133 to 393 K at 10 K/min. The glass-transition temperature, *T*_g, was taken as the midpoint of the heat capacity change at the transition from the amorphous to the liquid state.

Raman spectra were recorded on a Bruker IFS66 Fourier transform spectrometer equipped with a FRA106 Raman

module. The 1064 nm line of a Nd:YAG laser was used as the excitation source. The laser power was set to 200 mW, the resolution was 2 cm^{−1}, and the spectra were obtained as the average of ≥1000 scans. All of the Raman spectra were recorded at room temperature.

Quantum chemical calculations were performed with Gaussian 09 software.²⁷ An initial screening of four (MeO)(H)PO₂[−] and seven (EtO)(H)PO₂[−] structures at the HF/6-31G(d) computational level resulted in two stable and structurally unique anion conformers for each species. To take the effects of electron correlation into account, the structures were further optimized with the MP2/6-311+G(d) and B3LYP/6-311+G(d) approaches. The minimum-energy conformations were used as the input, and the MP2 potential-energy scans were performed to locate the barriers to rotation by rotating the O–P–O–R dihedral angles 360° in steps of 10° and allowing the remaining degrees of freedom to be optimized at each step.

The vibrational properties were calculated based on the B3LYP structures and used as the input for simulated Raman spectra. The calculated Raman activities were corrected for the scattering intensity dependence on the vibrational frequency. To ease the comparison of the calculated and experimental spectra, a Lorentzian broadening of 4 cm^{−1} (half-width at half-maximum) was applied to the discrete Raman shifts. To investigate the effect of ion–ion interactions on the Raman spectra of the isolated species, 10 ion-pair models of EMIm⁺(MeO)(H)PO₂[−] were optimized at the level of B3LYP/6-311+G(d), resulting in seven unique configurations. The most stable structures of EMIm⁺(MeO)(H)PO₂[−] were also used to guide the structural optimization of the DiMIm⁺(MeO)(H)PO₂[−] and EMIm⁺(EtO)(H)PO₂[−] ion pairs. The relative EMIm⁺–anion interaction strengths reported in the Results and Discussion section are for ion-pair structures optimized at the level of B3LYP/6-311+G(d).

3. RESULTS AND DISCUSSION

3.1. Phase Behavior. The DSC thermograms of the three phosphonate-based ILs are shown in Figure 2 together with the

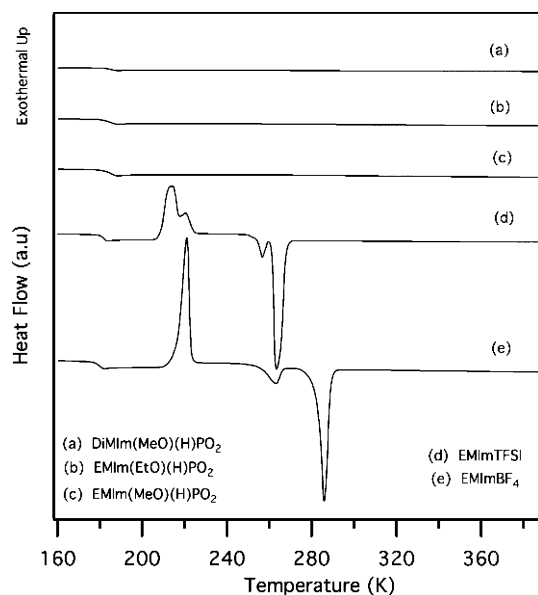


Figure 2. DSC traces of the five ionic liquids studied.

results for EMImTFSI and EMImBF₄. The phase behavior of EMImTFSI and EMImBF₄ is quite similar, with both showing a glass transition, a cold crystallization, and a solid–solid phase transition prior to melting. The phosphonate anion-based ILs, however, are stable toward crystallization, and only a glass transition is observed when using this protocol. (A cooling rate of 20 K/min and a heating rate of 10 K/min were used in the DSC experiments.) In fact, there is no crystallization observed for the phosphonate-based ionic liquids even when a lower cooling rate is used (5 K/min, data not shown). This is in contrast to that observed for EMImTFSI and EMImBF₄, where crystallization is found for the lower cooling rate.

If the IL anion is organic and there are conformational degrees of freedom, then the corresponding ILs generally show low melting points or only a glass-transition temperature.²⁸ Both of these requirements are met by the phosphonate anions. The conformational behavior is further discussed in section 3.3. The cation also plays a major role in the phase behavior of the ILs. Many ILs with the small and symmetric DiMIm cation, where DiMIm is 1,3-dimethylimidazolium, show relatively high melting points (T_m). For example, the T_m of DiMImBF₄ is 373 K²⁹ and that of DiMImTFSI is 299 K.¹⁶ However, DiMIm(MeO)(H)PO₂ does not crystallize easily, resulting in a very wide liquid range (trace a in Figure 2). The asymmetric structure of the phosphonate anions and the presence of several conformations are likely to result in poor packing of the ions in these ILs, preventing crystallization.

The glass-transition temperatures (T_g) of the investigated ILs are summarized in Table 1. Changing the alkyl group on the

Table 1. Glass-Transition Temperature (T_g), Ionic Conductivity at 298 K, and VFT Parameters of Ionic Conductivity (Fragility Parameter (D) and Ideal Glass Transition Temperature (T_0))

ionic liquid	T_g (K)	$\sigma_{298\text{ K}}$ (mS cm ⁻¹)	T_0 (K)	D
DiMIm(MeO)(H)PO ₂	184	7.25	174	4
EMIm(MeO)(H)PO ₂	185	4.87	168	4.7
EMIm(EtO)(H)PO ₂	185	5.34	164	5
EMImTFSI	182	9.15	187	2.2
EMImBF ₄	179	15.92	185	2.1

phosphonate anion (i.e., from methyl to ethyl) does not change T_g . The influence on T_g of the cation (DiMIm or EMIm) is also weak. However, the T_g of the phosphonate anion-based ILs is slightly higher compared to that of the BF₄⁻ and TFSI analogues. This difference in T_g can be attributed to the possibility of the phosphonate anions coordinating to the cation in many different configurations, as discussed below.

3.2. Ionic Conductivity. The ionic conductivity of imidazolium cation-based ILs has in general been extensively studied.^{12,15,16} However, according to our knowledge there are no reports on the conductivity of ILs based on imidazolium cations and phosphonate anions. The temperature dependence of the ionic conductivity of these ILs is shown in Figure 3 together with the corresponding data from EMImTFSI and EMImBF₄, and the conductivity values at room temperature (298 K) are summarized in Table 1. For EMImTFSI and EMImBF₄, which easily crystallize, data is shown only down to the melting points of 263 and 286 K, respectively. The room-temperature conductivity of EMImBF₄ is in excellent agreement with the literature value reported for a material with very low water content (<3 ppmw H₂O),³⁰ whereas the value for

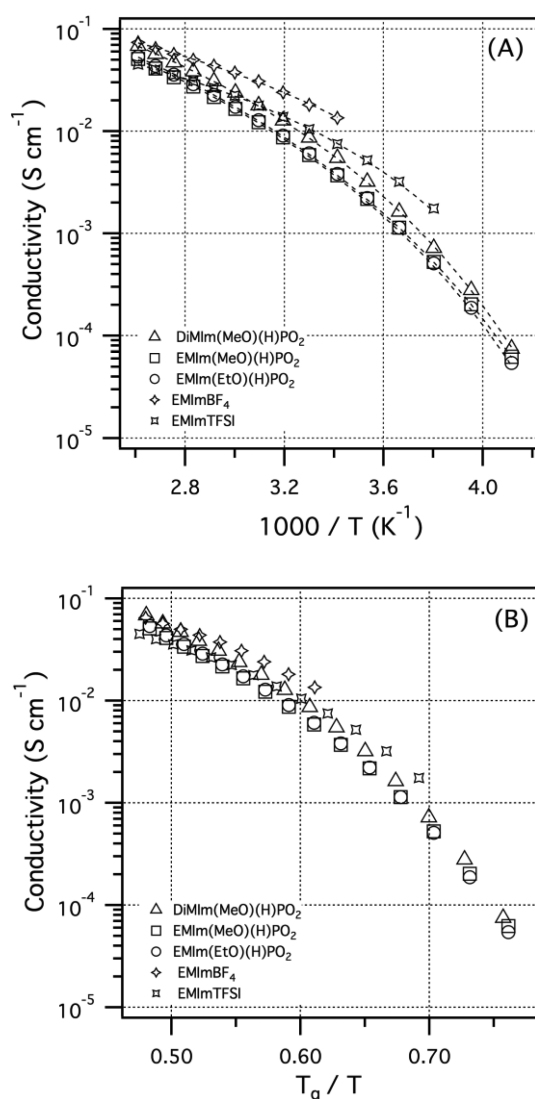


Figure 3. (A) Ionic conductivity as a function of the inverse temperature. Dashed lines are fits to the VFT equation (eq 1). For comparison, the ionic conductivities of EMImBF₄ and EMImTFSI are also included. (B) T_g -scaled ionic conductivity of the same ionic liquids.

EMImTFSI is slightly higher than what is reported in ref 31 (<2 ppmw H₂O).

All three phosphonate ILs show high conductivities, with DiMIm(MeO)(H)PO₂ having the highest value of 7.3×10^{-3} S cm⁻¹ at 298 K (Table 1). However, the conductivities are slightly lower than for the BF₄⁻ and TFSI analogues. The temperature dependence of the conductivity shows the typical non-Arrhenius behavior and is well described by the VFT (Vogel–Fulcher–Tammann) equation^{4,5,32}

$$\sigma = \sigma_0 e^{-DT_0/T - T_0} \quad (1)$$

where σ_0 is the conductivity at an infinitely high temperature, D relates to the fragility of the material, and T_0 is related to an ideal glass-transition temperature.³³ The D and T_0 values obtained from the ionic conductivity fits to eq 1 are reported in Table 1.

There is a small change in the VFT parameters among the different phosphonate ILs. The change in the D value can be related to a change in the fragility with the size of the ions.

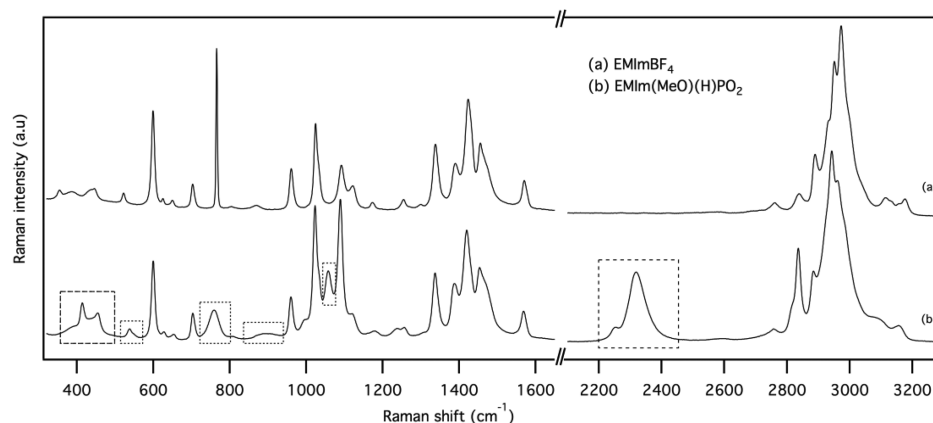


Figure 4. Raman spectra of EMImBF₄ and [EMIm(MeO)(H)PO₂] at 298 K. Regions with Raman signatures of the methyl-phosphonate anion are highlighted by dashed boxes. There are no bands in the range of 1650–2100 cm^{−1}; therefore, this region is not included.

However, the D values are considerably higher compared to those for EMImTFSI and EMImBF₄. This indicates that the fragilities of the ILs are influenced by the anion when comparing phosphonate anions to the BF₄[−] and TFSI anions. The flexible cation-coordinating ability of the phosphonate anions and the comparatively strong interactions with the cations should have an effect on the fragility of the ILs (i.e., the phosphonate ILs are less fragile compared to those with the BF₄[−] and TFSI anions). The calculated order of cation–anion interaction strengths in EMIm-based ionic liquids is, for example, TFSI (76 kcal/mol) < BF₄[−] (84 kcal/mol) < (EtO)(H)PO₂[−] (93 kcal/mol) \approx (MeO)(H)PO₂[−] (94 kcal/mol) at the level of B3LYP, which correlates well with the trend observed in the fragility. We note that a similar D value (around 4) was also found for the protic ionic liquid EMImTFSI (*N*-ethylimidazolium bis(trifluoromethanesulfonyl) imide), where hydrogen bonding contributes to the interaction.³⁴ We also note that the T_0 values are higher than the T_g values for the BF₄[−] and TFSI ILs. The reason for this behavior (i.e., whether it is a real effect or an effect of the smaller fitting region) is not clear. A similar result was reported for the [bpy][BF₄] (T_g = 188 K, T_0 = 189 K) and [b3mpy][N(CN)₂] (T_g = 185 K, T_0 = 187 K) ILs, where [bpy] is 1-butylpyridinium and [b3mpy] is 1-butyl-3-methylpyridinium.³⁵

To investigate further the relation between the ionic conductivity and the glass-transition temperature, the conductivity data are plotted with a T_g -scaled temperature axis, T_g/T , in Figure 3B. From this figure, it is clear that the data does not fall on a master curve and that there are other factors, in addition to the glass-transition temperature, controlling the conductivity. Following the trend found in the D parameter this plot further underscores that the ionic conductivities do not have the same temperature dependence and that the fragility of the studied ILs differs.

3.3. Structure and Interactions. The structure of various anions in imidazolium-based ionic liquids has previously been investigated using Raman spectroscopy and quantum chemical calculations.^{36–39} However, to our knowledge there are no Raman data reported for the phosphonate anion as part of ILs.

The experimental Raman spectrum of 1-ethyl-3-methylimidazolium methyl-phosphonate [EMIm(MeO)(H)PO₂] is shown in Figure 4. To identify signatures from the methyl-phosphonate anion (dashed boxes), the Raman spectrum of EMImBF₄ is also included in the figure. In Figure 5, the experimental Raman spectrum of [EMIm(MeO)(H)PO₂] ionic

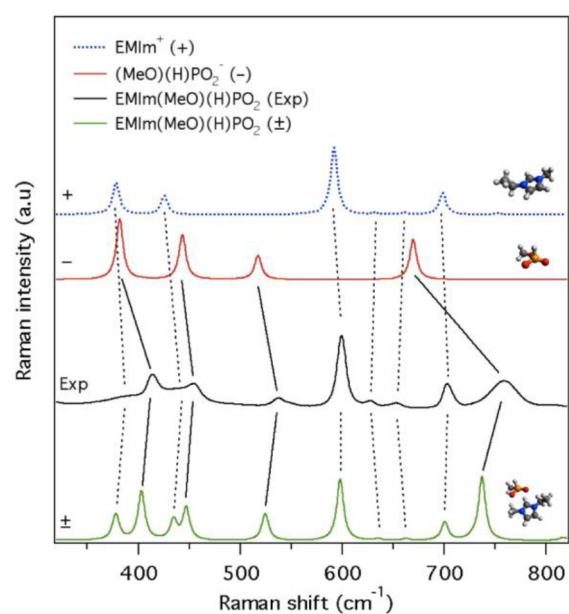


Figure 5. Simulated Raman spectra of EMIm⁺ (+), (MeO)(H)PO₂[−] (−), and EMIm(MeO)(H)PO₂ (±) at computational level B3LYP/6-311+G(d) are compared to the experimental Raman spectrum of EMIm(MeO)(H)PO₂.

liquid is compared to the simulated spectra of the [EMIm(MeO)(H)PO₂] ion pair and the isolated cation and anion. This comparison reveals that for the phosphonate anion-based ILs it is important to take into account the ion–ion interactions to correctly reproduce the experimental spectrum. In the highlighted wavenumber region of Figure 5, it is possible to determine the anionic and cationic contributions to the experimental spectrum for most of the bands by resorting only to simulated spectra of the isolated cation (+) and anion (−). However, as evidenced for several anion bands and most clearly observed for the experimental ~ 750 cm^{−1} envelope of bands, the position of the calculated band is strongly influenced by the structural model. The correspondence of the simulated and experimental spectra is considerably improved using an ion-pair model. Although the correspondence may be improved further by modeling larger ionic aggregates,⁴⁰ the ion-pair model is used as an adequate representation for the systems studied here.

The vibrational spectroscopic and computational studies on different phosphonate and phosphite compounds can be found in the literature,^{41–47} and the vibrational frequencies of neutral dialkyl phosphonates, $(\text{RO})_2\text{P}(\text{O})\text{H}$ (R-alkyl group), have been reported. The phosphonate anions used here, with the exception of having only one methoxy or ethoxy group bonded to the central P atom, are very similar and can be compared with the dialkyl phosphonates. The literature data also report the presence of different conformers of the phosphonate compounds.^{43–45,47} By taking this into account, we first investigate the anion conformations in section 3.3.1 and then discuss the different anionic vibrational modes in section 3.3.2.

3.3.1. Anion Conformations. The conformational isomerism of phosphonate compounds is a result of the rotation about the O–R bonds.^{42–44,47} The number of conformations depends on the type and number of alkyl groups. Georgiev et al. reported three stable conformers of the methyl-phosphonate anion, with two of the conformers being mirror images having global minima of -0.6 kcal/mol each compared to a third conformer.⁴² In Figure 6, the conformational-energy landscape

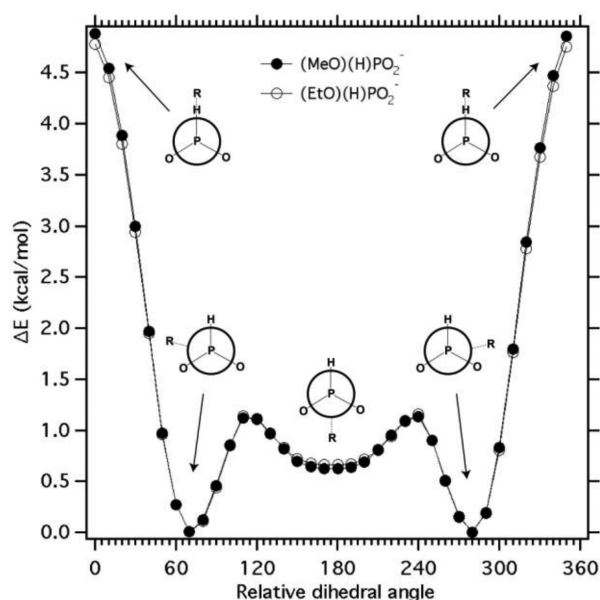


Figure 6. Conformational-energy landscape of $(\text{MeO})(\text{H})\text{PO}_2^-$ and $(\text{EtO})(\text{H})\text{PO}_2^-$ as a function of the dihedral angle O–P–O–C relative to the angle at the energy maxima. Newman projections of the methyl-phosphonate anion are included for the energy minima and the high energy maximum.

of the phosphonate anions is depicted as a function of the dihedral angle O–P–O–C relative to the angle at the energy maxima. The results for the methyl- and ethyl-phosphonates are close to identical, indicating that there is no preference for a methyl or ethyl group along this coordinate of the potential-energy surface. Moreover, the calculated methyl-phosphonate conformational-energy difference, 0.51 and 0.62 kcal/mol at the B3LYP and MP2 levels, respectively, is close to the result obtained by Georgiev et al.⁴²

According to the potential-energy landscape in Figure 6, the transition between the two global minima can occur directly or alternatively via the higher-energy conformer, with the latter being the energetically preferred route. The barriers to the conformational isomerization of methyl-phosphonate have been calculated to be 4.92 and 1.14 kcal/mol, respectively, on

the basis of the energies of the transition states with respect to the global minima at the level of MP2. In comparison to that of EMIm^+ , for which the maximum and minimum barriers to rotation are approximately 1.5 and 0.7 kcal/mol,⁴⁸ the rotation around the O–R bonds in the phosphonates are suggested to be much more restricted. However, the minimum-energy path between the two distinct conformers should be almost as facile as for that of EMIm^+ , where the two cation conformers have been found to coexist at room temperature in several ILs.^{48,36} Thus, a similar coexistence of anion conformers in the phosphonate ionic liquids is plausible. For the related dialkyl phosphite molecular liquids, several different phosphonate conformers have been identified using IR and Raman spectroscopy in the liquid and crystalline states or in solution.⁴³ The spectral changes in these systems have been most clearly manifested in the P–H stretching vibration.

3.3.2. Vibrational Spectra. From a comparison of the experimental reference spectra (EMImBF_4 and EMImTFSI) and with the aid of simulated spectra, several regions with clear Raman bands from the anion have been identified for the three phosphonate-based ILs (Figure 7). Selected anion vibrational frequencies and their corresponding mode assignments are presented in Table 2.

We observe that the experimental and calculated Raman signatures of the anion show a dependence on the position and shape of the cation species as well as of the alkyl group on the anion. To differentiate the three oxygen atoms in the anions, they are labeled according to Figure 1. The O(1) and O(1*) atoms are distinguishable only when considering specific conformers, as exemplified by calculations suggesting that the P–O(1) and P–O(1*) bond lengths are roughly equal and with more double-bond than single-bond character.⁴² Here, an asterisk is used to highlight that the O(1*) atom is closer to the alkyl group than the O(1) atom.

The shape of the bands belonging to the O–P–O bending modes^{44,46} of the $(\text{MeO})(\text{H})\text{PO}_2^-$ anion in the 380–500 cm^{-1} region are somewhat similar to those of the two ILs based on this anion, whereas the shape of this spectral region is considerably different for the $(\text{EtO})(\text{H})\text{PO}_2^-$ anion-based IL. This indicates that the alkyl group attached to the O(2) atom influences these vibrations considerably. The most evident shift of the high-wavenumber component at 455 cm^{-1} in $\text{EMIm}-(\text{MeO})(\text{H})\text{PO}_2$ to 469 cm^{-1} in $\text{EMIm}(\text{EtO})(\text{H})\text{PO}_2$ is confirmed by the calculated data. The position of the band found at 520–570 cm^{-1} shifts only for $(\text{EtO})(\text{H})\text{PO}_2^-$, which again indicates the dependence of the alkyl group attached to the O(2) atom. Moreover, in both of these regions the shapes of spectra a and b are somewhat different, indicating the cation influence on the vibrational modes of the anion.

The influence of the alkyl group attached to the O(2) atom on the anion vibrations are also clearly visible in the 680–820 cm^{-1} region. In spectra b and c, the ILs share the same cation, only the anion is changed. The P–O(2) stretching vibration found at ~ 760 cm^{-1} for $(\text{MeO})(\text{H})\text{PO}_2^-$ has split into several components for $(\text{EtO})(\text{H})\text{PO}_2^-$. The calculated results predict only one component for either anion conformer (Table 2), which suggests the presence of different anion conformers in the ionic liquid. The calculated shift for a change in $(\text{EtO})(\text{H})\text{PO}_2^-$ conformation within the ion-pair model is $\Delta\nu = -24$ cm^{-1} , in good agreement with the 25 cm^{-1} difference of the strongest (777 cm^{-1}) and second strongest (752 cm^{-1}) experimental signatures of the $\text{EMIm}(\text{EtO})(\text{H})\text{PO}_2$ spectrum (Table 2). However, the broad features of the experimental

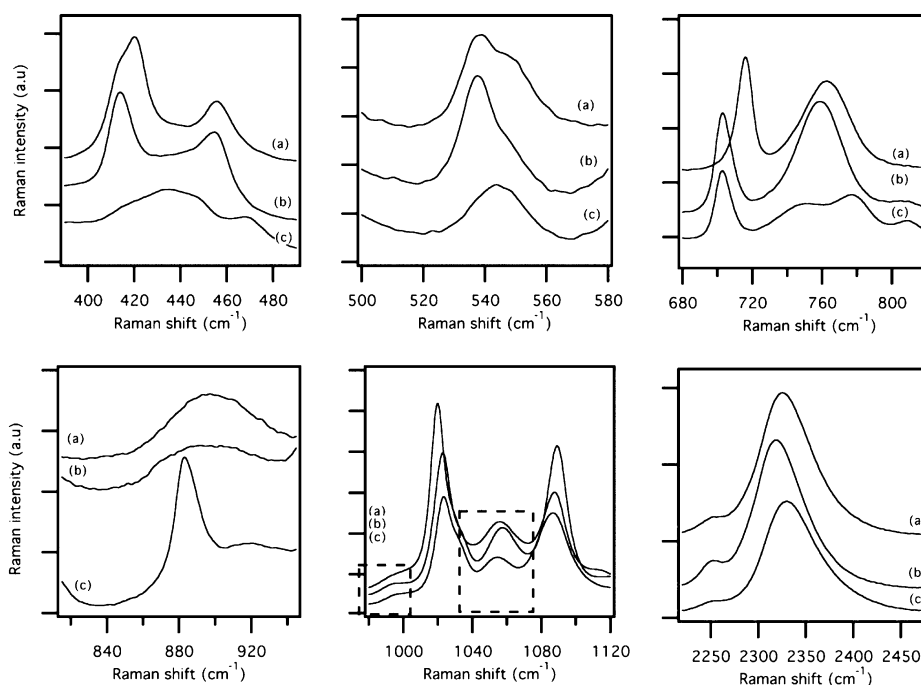


Figure 7. Raman spectra of [DiMIm(MeO)(H)PO₂][−], (a); [EMIm(MeO)(H)PO₂][−], (b); and [EMIm(EtO)(H)PO₂][−], (c).

Table 2. Experimental and Calculated Frequencies and Mode Assignments for the Alkyl-Phosphonate Anions

(MeO)(H)PO ₂ ^a		(MeO)(H)PO ₂ ^b		(EtO)(H)PO ₂		$\Delta\nu^d$	assignment ^e
exp	cal ^c	exp	cal ^c	exp	cal ^c		
420	402	414	403	434	396	−4/−3/4	δ [O(2)–P–O(1)]
456	446	455	447	469	465	8/6/7	δ_{oph} [O(2)–P–O(1*); C–O(2)–P]
536	525	536	525	544	528	35/35/35	π [PO ₃]
763	738	759	737	752	762	−18/−17/−24	ν [P–O(2)]
				777			
				883	939	−5	ν_s [C–C; C–O(2)]
995	995	995	996	995	995	−5/−4/6	δ [H–P–O(2)]
1056	1058	1057	1059	1054	1055	−9/−10/−8	ν_s [P–O(1*); P–O(1)]
							ν_{as} [O(2)–C; O(2)–P]
2326	2371	2320	2373	2330	2370	66/60/61	ν [P–H]

^a1,3-Dimethylimidazolium methyl-phosphonate. ^b1-Ethyl-3-methylimidazolium methyl-phosphonate. ^cRaman shifts calculated for ion-pair models using B3LYP/6-311+G(d). ^d $\Delta\nu$ is the calculated shift in the vibrational wavenumber of the second-most-stable anion conformer relative the most stable in the respective ion-pair models. ^e δ = bending, δ_{oph} = out-of-phase bending, π = inversion, ν = stretching, ν_s = symmetric stretching, and ν_{as} = asymmetric stretching.

spectrum and the additional $\sim 810\text{ cm}^{-1}$ component indicate that the origin of the experimental bands is more complex than what can be described by a simple model using only two anion conformers, as discussed below. Once again there is a slight change of the band positions as a function of the cation (spectra a and b). The origin of the broad features found in the $840\text{--}940\text{ cm}^{-1}$ region of the (MeO)(H)PO₂[−] anion is not clear. However, a sharp low-frequency peak of the (EtO)(H)PO₂[−] anion can be found at 883 cm^{-1} , which is assigned to a combination of symmetric C–C and C–O(2) vibrations. The bending mode of H–P–O(2) can be found at the same position, 995 cm^{-1} , for both anions.

Among the anion bands, the shape and position of the bands in the $1040\text{--}1080\text{ cm}^{-1}$ region are quite similar for all ILs. The band centered at $\sim 1055\text{ cm}^{-1}$ is assigned to a symmetric combination of the P–O(1*) and P–O(1) stretching modes and an asymmetric combination of O(2)–C and O(2)–P vibrations. The broad and highly intense Raman bands at

$2200\text{--}2450\text{ cm}^{-1}$ are characteristic of the P–H stretch.^{41,43,46,47} Overall, the three experimental bands at ~ 540 , ~ 760 , and 2350 cm^{-1} , which show very broad features from multiple contributions, are also the bands computationally predicted to be affected the most by a change in the anion conformation (Table 2). However, the presence of only two different anion conformers is not enough to explain the experimental features. In addition to the conformational flexibility of both the anion and cation, a distribution of cation–anion coordination configurations (i.e., changes in the local environment of the anions) is a possible explanation for the results. In fact, the computational results suggest a large number of stable anion–cation configurations where the anion can interact with any of the cation protons via either of the anion oxygen atoms. However, a more detailed discrimination of the different contributions of the anion bands is beyond the scope of this work. For the related molecular liquids, the alkyl-phosphite and alkyl-phosphonate compounds, similar peak broadening has

been attributed to the formation of dimeric structures⁴⁹ as a result of intermolecular interactions between the P–H proton of one molecule with the oxygen atoms of a neighboring molecule. However, for the ionic compounds here, repulsion of the negative charges disfavor the formation of such structures. Therefore, the relation of the spectral broadening to any type of hydrogen-bonded anion clusters is unlikely.

4. CONCLUSIONS

In this Article, we report the ionic conductivities, phase behaviors, interactions, and structures of anions of ionic liquids based on phosphonate anions and imidazolium cations. The influence of the phosphonate anions on the IL properties is explored by comparing the results with those of the corresponding ILs featuring the two well-established anions, BF_4^- and TFSI. All ILs show high ionic conductivities of around $10^{-3} \text{ S cm}^{-1}$ at 298 K. A clear anion effect on the glass-transition temperature and fragility is observed when going from the phosphonate anions to BF_4^- and TFSI. This behavior is attributed to the ability of the phosphonate anions to form a large number of complexes with the cation. This ability is also evident in the broad, multiple-component anion vibrational bands identified from Raman spectroscopy. In addition, the spectroscopic data show that the phosphonate-anion vibrational modes are clearly influenced by the alkyl group on the anion and the type of the IL cation. The results of ab initio calculations enable the assignment of anion vibrational bands and provide insight into the energetics of anion conformational change. Two different barriers to rotation are found between the two unique stable conformations of both the methyl-phosphonate and ethyl-phosphonate anions, favoring isomerism in a restricted rotational space.

AUTHOR INFORMATION

Corresponding Author

*E-mail: matic@chalmers.se. Fax: +46317722090.

Notes

The authors declare no competing financial interest.

ACKNOWLEDGMENTS

This work was supported by Chalmers Areas of Advance Materials Science and Energy and the Swedish Research Council.

REFERENCES

- (1) Wilkes, J. S. A Short History of Ionic Liquids—from Molten Salts to Neoteric Solvents. *Green Chem.* **2002**, *4*, 73–80.
- (2) Ohno, H. Importance and Possibility of Ionic Liquids. In *Electrochemical Aspects of Ionic Liquids*; Ohno, H., Ed.; John Wiley & Sons, Inc.: Hoboken, NJ, 2005; pp 1–3.
- (3) Dzyuba, S. V.; Bartsch, R. A. Influence of Structural Variations in 1-Alkyl(aralkyl)-3-methylimidazolium Hexafluorophosphates and Bis-(trifluoromethylsulfonyl)imides on Physical Properties of the Ionic Liquids. *ChemPhysChem.* **2002**, *3*, 161–166.
- (4) Tokuda, H.; Hayamizu, K.; Ishii, K.; Susan, M. A. B. H.; Watanabe, M. Physicochemical Properties and Structures of Room Temperature Ionic Liquids. 2. Variation of Alkyl Chain Length in Imidazolium Cation. *J. Phys. Chem. B* **2005**, *109*, 6103–6110.
- (5) Tokuda, H.; Ishii, K.; Susan, M. A. B. H.; Tsuzuki, S.; Hayamizu, K.; Watanabe, M. Physicochemical Properties and Structures of Room-Temperature Ionic Liquids. 3. Variation of Cationic Structures. *J. Phys. Chem. B* **2006**, *110*, 2833–2839.
- (6) Anderson, J. L.; Ding, R.; Ellern, A.; Armstrong, D. W. Structure and Properties of High Stability Geminal Dicationic Ionic Liquids. *J. Am. Chem. Soc.* **2005**, *127*, 593–604.
- (7) Appetecchi, G. B.; Montanino, M.; Zane, D.; Carewska, M.; Alessandrini, F.; Passerini, S. Effect of the Alkyl Group on the Synthesis and the Electrochemical Properties of N-Alkyl-N-methylpyrrolidinium bis(trifluoromethanesulfonyl)imide Ionic Liquids. *Electrochim. Acta* **2009**, *54*, 1325–1332.
- (8) MacFarlane, D. R.; Pringle, J. M.; Johansson, K. M.; Forsyth, S. A.; Forsyth, M. Lewis Base Ionic Liquids. *Chem. Commun.* **2006**, 1905–1917.
- (9) Ueno, K.; Tokuda, H.; Watanabe, M. Ionicity in Ionic Liquids: Correlation with Ionic Structure and Physicochemical Properties. *Phys. Chem. Chem. Phys.* **2010**, *12*, 1649–1658.
- (10) Zhou, Z.-B.; Matsumoto, H.; Tatsumi, K. Structure and Properties of New Ionic Liquids Based on Alkyl- and Alkenyltrifluoroborates. *ChemPhysChem.* **2005**, *6*, 1324–1332.
- (11) Noda, A.; Hayamizu, K.; Watanabe, M. Pulsed-Gradient Spin-Echo ^1H and ^{19}F NMR Ionic Diffusion Coefficient, Viscosity, and Ionic Conductivity of Non-Chloroaluminate Room-Temperature Ionic Liquids. *J. Phys. Chem. B* **2001**, *105*, 4603–4610.
- (12) Matsumoto, H.; Kageyama, H.; Miyazaki, Y. Room Temperature Ionic Liquids Based on Small Aliphatic Ammonium Cations and Asymmetric Amide Anions. *Chem. Commun.* **2002**, 1726–1727.
- (13) Tokuda, H.; Hayamizu, K.; Ishii, K.; Susan, M. A. B. H.; Watanabe, M. Physicochemical Properties and Structures of Room Temperature Ionic Liquids. 1. Variation of Anionic Species. *J. Phys. Chem. B* **2004**, *108*, 16593–16600.
- (14) Kunze, M.; Jeong, S.; Paillard, E.; Winter, M.; Passerini, S. Melting Behavior of Pyrrolidinium-Based Ionic Liquids and Their Binary Mixtures. *J. Phys. Chem. C* **2010**, *114*, 12364–12369.
- (15) Seki, S.; Kobayashi, T.; Kobayashi, Y.; Takei, K.; Miyashiro, H.; Hayamizu, K.; Tsuzuki, S.; Mitsugi, T.; Umebayashi, Y. Effects of Cation and Anion on Physical Properties of Room-Temperature Ionic Liquids. *J. Mol. Liq.* **2010**, *152*, 9–13.
- (16) Tokuda, H.; Tsuzuki, S.; Susan, M. A. B. H.; Hayamizu, K.; Watanabe, M. How Ionic Are Room-Temperature Ionic Liquids? An Indicator of the Physicochemical Properties. *J. Phys. Chem. B* **2006**, *110*, 19593–19600.
- (17) Wasserscheid, P.; Hal, R. V.; Bösmann, A. 1-*n*-Butyl-3-methylimidazolium ([bmim]) Octylsulfate—An Even ‘Greener’ Ionic Liquid. *Green Chem.* **2002**, *4*, 400–404.
- (18) Shah, F. U.; Glavatskih, S.; MacFarlane, D. R.; Somers, A.; Forsyth, M.; Antzutkin, O. N. Novel Halogen-Free Chelated Orthoborate-Phosphonium Ionic Liquids: Synthesis and Tribophysical Properties. *Phys. Chem. Chem. Phys.* **2011**, *13*, 12865–12873.
- (19) Bonhôte, P.; Dias, A.-P.; Papageorgiou, N.; Kalyanasundaram, K.; Grätzel, M. Hydrophobic, Highly Conductive Ambient-Temperature Molten Salts. *Inorg. Chem.* **1996**, *35*, 1168–1178.
- (20) Henderson, W. A.; Passerini, S. Phase Behavior of Ionic Liquid-LiX Mixtures: Pyrrolidinium Cations and TFSI-Anions. *Chem. Mater.* **2004**, *16*, 2881–2885.
- (21) Martinelli, A.; Matic, A.; Jacobsson, P.; Börjesson, L. Phase Behavior and Ionic Conductivity in Lithium Bis-(trifluoromethanesulfonyl)imide-Doped Ionic Liquids of the Pyrrolidinium Cation and Bis(trifluoromethanesulfonyl)imide Anion. *J. Phys. Chem. B* **2009**, *113*, 11247–11251.
- (22) Zhou, Q.; Fitzgerald, K.; Boyle, P. D.; Henderson, W. A. Phase Behavior and Crystalline Phases of Ionic Liquid-Lithium Salt Mixtures with 1-Alkyl-3-methylimidazolium Salts. *Chem. Mater.* **2010**, *22*, 1203–1208.
- (23) Kuhlmann, E.; Himmler, S.; Giebelhaus, H.; Wasserscheid, P. Imidazolium Dialkylphosphates—A Class of Versatile, Halogen-Free and Hydrolytically Stable Ionic Liquids. *Green Chem.* **2007**, *9*, 233–242.
- (24) Nishi, N.; Kawakami, T.; Shigematsu, F.; Yamamoto, M.; Kakiuchi, T. Fluorine-Free and Hydrophobic Room-Temperature Ionic Liquids, Tetraalkylammonium Bis(2-ethylhexyl)sulfosuccinates,

and Their Ionic Liquid–Water Two-Phase Properties. *Green Chem.* **2006**, *8*, 349–355.

(25) Hasse, B.; Lehmann, J.; Assenbaum, D.; Wasserscheid, P.; Leipertz, A.; Fröba, A. P. Viscosity, Interfacial Tension, Density, and Refractive Index of Ionic Liquids [EMIM][MeSO₃], [EMIM][MeOHPO₂], [EMIM][O₂CSO₄], and [BBIM][NTf₂] in Dependence on Temperature at Atmospheric Pressure. *J. Chem. Eng. Data* **2009**, *54*, 2576–2583.

(26) Sun, J.; Howlett, P. C.; MacFarlane, D. R.; Lin, J.; Forsyth, M. Synthesis and Physical Property Characterisation of Phosphonium Ionic Liquids Based on P(O)₂(OR)₂[−] and P(O)₂(R)₂[−] Anions with Potential Application for Corrosion Mitigation of Magnesium Alloys. *Electrochim. Acta* **2008**, *54*, 254–260.

(27) Frisch, M. J.; Trucks, G. W.; Schlegel, H. B.; Scuseria, G. E.; Robb, M. A.; Cheeseman, J. R.; Scalmani, G.; Barone, V.; Mennucci, B.; Petersson, G. A., et al. *Gaussian 09*, revision A.1; Gaussian, Inc.: Wallingford, CT, 2009.

(28) Ohno, H. Functional Design of Ionic Liquids. *Bull. Chem. Soc. Jpn.* **2006**, *79*, 1665–1680.

(29) Holbrey, J. D.; Seddon, K. R. The Phase Behaviour of 1-Alkyl-3-methylimidazolium Tetrafluoroborates; Ionic Liquids and Ionic Liquid Crystals. *J. Chem. Soc., Dalton Trans.* **1999**, 2133–2139.

(30) Schreiner, C.; Zugmann, S.; Hartl, R.; Gores, H. J. J. Fractional Walden Rule for Ionic Liquids: Examples from Recent Measurements and a Critique of the So-Called Ideal KCl Line for the Walden Plot. *Chem. Eng. Data* **2010**, *55*, 1784–1788.

(31) Appetecchi, G. B.; Montanino, M.; Carewska, M.; Moreno, M.; Alessandrini, F.; Passerini, S. Chemical-Physical Properties of Bis-(perfluoroalkylsulfonyle)imide-Based Ionic Liquids. *Electrochim. Acta* **2011**, *56*, 1300–1307.

(32) Leys, J.; Wübbenhorst, M.; Menon, C. P.; Rajesh, R.; Thoen, J.; Glorieux, C.; Nockemann, P.; Thijs, B.; Binnemans, K.; Longuemart, S. Temperature Dependence of the Electrical Conductivity of Imidazolium Ionic Liquids. *J. Chem. Phys.* **2008**, *128*, 064509-1–064509-7.

(33) Tamman, G.; Hesse, W. Z. The Dependency of Viscosity on Temperature in Hypothermic Liquids. *Z. Anorg. Allg. Chem.* **1926**, *156*, 245–257.

(34) Martinelli, A.; Matic, A.; Jacobsson, P.; Börjesson, L.; Fericola, A.; Panero, S.; Scorsati, B.; Ohno, H. Physical Properties of Proton Conducting Membranes Based on a Protic Ionic Liquid. *J. Phys. Chem. B* **2007**, *111*, 12462–12467.

(35) Bandrés, I.; Montañó, D. F.; Gascón, I.; Cea, P.; Lafuente, C. Study of the Conductivity Behavior of Pyridinium-Based Ionic Liquids. *Electrochim. Acta* **2010**, *55*, 2252–2257.

(36) Lassègues, J. C.; Grondin, J.; Holomb, R.; Johansson, P. Raman and Ab Initio Study of the Conformational Isomerism in the 1-Ethyl-3-methyl-imidazolium Bis(trifluoromethanesulfonyl)imide Ionic Liquid. *J. Raman Spectrosc.* **2007**, *38*, 551–558.

(37) Ribeiro, M. C. High Viscosity of Imidazolium Ionic Liquids with the Hydrogen Sulfate Anion: A Raman Spectroscopy Study. *J. Phys. Chem. B* **2012**, *116*, 7281–7290.

(38) Jeon, Y.; Sung, J.; Seo, C.; Lim, H.; Cheong, H.; Kang, M.; Moon, B.; Ouchi, Y.; Kim, D. Structures of Ionic Liquids with Different Anions Studied by Infrared Vibration Spectroscopy. *J. Phys. Chem. B* **2008**, *112*, 4735–4740.

(39) Grondin, J.; Lassègues, J. C.; Cavagnat, D.; Buffeteau, T.; Johansson, P.; Holomb, R. Revisited Vibrational Assignments of Imidazolium-Based Ionic Liquids. *J. Raman Spectrosc.* **2011**, *42*, 733–743.

(40) Angenendt, K.; Johansson, P. Ionic Liquid Based Lithium Battery Electrolytes: Charge Carriers and Interactions Derived by Density Functional Theory Calculations. *J. Phys. Chem. B* **2011**, *115*, 7808–7813.

(41) Doak, G. O.; Freedman, L. D. The Structure and Properties of the Dialkyl Phosphonates. *Chem. Rev.* **1961**, *61*, 31–44.

(42) Georgiev, E. M.; Kaneti, J.; Troev, K.; Roundhill, D. M. An Ab-Initio Study of the Mechanism of the Atherton-Todd Reaction

Between Dimethyl Phosphonate and Chlorosubstituted and Fluoro-Substituted Methanes. *J. Am. Chem. Soc.* **1993**, *115*, 10964–10973.

(43) Katcyuba, S. A.; Monakhova, N. I.; Ashrafullina, L. Kh.; Shagidullin, R. R. Vibrational-Spectra, Conformations and Force-Constants of Dialkylphosphites (RO)₂P(O)H. *J. Mol. Struct.* **1992**, *269*, 1–21.

(44) Moravie, R. M.; Froment, F.; Corset, J. Vibrational-Spectra and Possible Conformers of Dimethylphosphonate by Normal Mode Analysis. *Spectrochim. Acta* **1989**, *45*, 1015–1024.

(45) Strajbl, M.; Baumruk, V.; Florián, J.; Bednárová, L.; Rosenberg, I.; Stepánek, J. Molecular Structure, Vibrational Spectra and Quantum Mechanical Force Fields of Modified Oligonucleotide Linkages: 1. Methyl Methoxymethanphosphonate. *J. Mol. Struct.* **1997**, *415*, 161–177.

(46) Carauta, A. N. M.; de Souza, V.; Hollauer, E.; Téllez, S. Vibrational Study of Dialkylphosphonates: Di-n-Propyl- and Di-i-Propylphosphonates by Semiempirical and Ab Initio Methods. *Spectrochim. Acta, Part A* **2004**, *60*, 41–51.

(47) Carauta, A. N. M.; de M. Carneiro, J. W.; Soto, C. A. T. Conformational and Vibrational Study of Di-n-Propyl and Di-i-Propylphosphonates by MM/QM Method. *Int. J. Quantum Chem.* **2005**, *103*, 763–774.

(48) Umebayashi, Y.; Fujimori, T.; Sukizaki, T.; Asada, M.; Fujii, K.; Kanzaki, R.; Ishiguro, S.-I. Evidence of Conformational Equilibrium of 1-Ethyl-3-methylimidazolium in Its Ionic Liquid Salts: Raman Spectroscopic Study and Quantum Chemical Calculations. *J. Phys. Chem. A* **2005**, *109*, 8976–8982.

(49) Meyrick, C. I.; Thompson, H. W. Vibrational Spectra of Alkyl Esters of Phosphorus Oxy-Acids. *J. Chem. Soc.* **1950**, 225–229.